https://doi.org/ 10.33472/AFJBS.6.9.2024.4664-4686

African Journal of Biological Sciences

Journal homepage: http://www.afjbs.com

Research Paper Open Access

Formulation and Evaluation of Chitosan-Based Polyelectrolyte Complex via Pulmonary Route by Anti-Convulsant drug Topiramate

Raviraj Ramrao More [1]*, Anup Kumar Chakraborty[2]

1. IES Institute of Pharmacy, IES University, Bhopal, M.P.
2. IES Institute of Pharmacy, IES University, Bhopal, M.P.

Article History: Volume 6,Issue 9, 2024

Received: 29 Apr 2024

Accepted : 18 May 2024

doi: 10.33472/AFJBS.6.9.2024.4664-4686

Abstract: Chitosan, which is biodegradable, biocompatible, non-toxic, and mucoadhesive, is frequently employed in the creation of nasal drug delivery nanoparticles that utilize polyelectrolyte complexes. Chitosan's usage in the pharmaceutical and biomedical industries is nevertheless constrained by its reduced solubility in aqueous and alkaline conditions. This necessitates the creation of enhanced chemically modified chitosan mimics that can get beyond the solubility barrier. Using a straightforward ionic gelation process, chitosan-based polyelectrolyte complexes (PEC) were created by the interaction of positively charged chitosan with negatively charged pectin. SEM was used to study the surface morphology and revealed that smooth and rough surfaces were created by varying the counter-ions, resulting in spheres or discs. DSC and FTIR were used to validate the development of the polyelectrolyte complex. As an oral tablet, topiramate is a second-generation antiepileptic medication used to treat partial and generalized seizures. Although it is more convenient, oral administration results in delayed absorption. Additionally, because parenteral administration necessitates medical support, it is impossible in emergency situations. In order to create topiramate PEC for intranasal delivery using the ionotropic gelation process, the current study has this objective. Particle size, zeta potential, surface shape, drug content, entrapment effectiveness, in vitro drug release, and ex vivo permeation experiments in excised porcine nasal mucosa were all examined for the produced PEC. Nasal mucosa was not harmed by the optimized formulation, according to investigations on rhinocilial toxicity. Thus, a promising alternative for brain targeting and the treatment of epilepsy is the intranasal administration of topiramate utilizing chitosan.

Keywords: Polyelectrolyte Complex, Anti-Convulsant, Topiramate, Pulmonary Route, Chitosan, etc.

Introduction

Recurrent seizures or episodes of strange behaviour, as well as occasionally losing consciousness, are hallmarks of the chronic neurological condition epilepsy [1,2]. Although the oral method of administration is the most practical for treating epilepsy, it plays a negligible part in treating an acute epileptic attack since oral medication has a delayed absorption. Additionally, because it requires medical help, parenteral administration is not an option in emergency situations. In order to get good results, a different medication delivery method is highly desirable [3,4]. Along with a porous and highly vascularized epithelium layer, the intranasal route offers a larger surface area for drug absorption. Additionally, there is more overall blood flow to the nasal region, which promotes quicker drug absorption and, thus, quicker beginning of effect. In addition to this, intranasal administration aids in the delivery of centrally active medications to the brain via the olfactory area and trigeminal nerves [5]. As a result, it is a practical and appropriate route of administration for the treatment of epilepsy [6].

In contrast, mucociliary clearance is the limiting factor that shortens the time a drug spends in the nasal cavity and, as a result, restricts the amount of drug absorption [7]. Making a dosage form containing a mucoadhesive ingredient will help you get over the mucociliary clearance restriction. The formulation's adhesion to the mucosal membrane will stop the medication from leaving the nasal cavity too quickly and give it more time to be absorbed, producing a therapeutic level that is high enough [8,9]. Chitosan, a naturally occurring polysaccharide with mucoadhesive, biodegradable, non-toxic, and biocompatible properties, has been selected in this context as the carrier for the synthesis of PEC [10]. The tight connections between the epithelial cells are also opened, which improves paracellular absorption [11]. The natural carbohydrate polymer chitosan (CS), which is made from chitin through a process called deacetylation, has several enticing qualities such being non-toxic, bioadhesive, and biodegradable. Due to the high rate of adhesion, it has the advantage of bypassing the body's natural defensive system known as mucociliary clearance while also displaying penetration-enhancing qualities that are extremely advantageous to chemotherapy. Chitosan's mucoadhesive activity results from its cationic nature, which interacts electrostatically with negatively charged pectin moieties on the mucosal membrane [12]. The PEC-based formulation offers targeted medication release with better absorption and action at the location. Additionally, pharmacological adverse effects related to traditional therapy are decreased by site-specific administration [13,14]. Drugs like lamotrigine and pregabalin have successfully improved mucoadhesion, release, and absorption using intranasal formulation of antiepileptic medicines with chitosan [15,16]. A second-generation antiepileptic medication called topiramate is used to treat both partial and generalised seizures. It is used as a preventative measure for obesity, psychological illnesses, and migraine headaches. Children who are experiencing refractory partial seizures with or without additional generalised tonic-clonic seizures can also be treated with topiramate [17,18]. There is currently no researched intranasal formulation for topiramate; it is only available in oral dose forms. Topiramate's rate of absorption is slowed when administered with meals, and cytochrome p450-mediated oxidation occurs [19,20].

The response surface methodology (RSM) is a collection of mathematical and statistical methods that have been successfully used for the process' development and optimisation [21]. RSM is a priceless technology that allows the influence of all independent variables to be examined with the fewest feasible experiments [22]. Since RSM is sophisticated and sensitive to the interactions of two or more elements, it is used in this study to explain how these interactions affect the development of the formulation and the properties of the topiramate PEC based on chitosan. In order to develop an optimised formulation with the most desirable physicochemical qualities sufficiently to produce

improved therapeutic effects, tests were conducted using a three factor and three-full level factorial design.

Material and Method

Preformulation Study
Identification of drug

Identification Topiramate was carried out by melting point determination, Infrared spectroscopy and UV visible spectroscopy.

Melting point determination

Melting point of the drug determined by taking small amount of drug in a capillary tube closed at one end. The capillary tube was placed in melting point apparatus and the temperature at which drug melt was recorded this procedure was performed thrice and average value was noted.

Determination of λ max and plotting of calibration curve of Topiramate in methanol

Accurately weighed 10 mg of Topiramate was dissolved in 10 ml of methanol to obtained 1000 µg/ml concentration of drug (stock solution), from stock solution to obtain concentrations of 10, 15, 20, 25 & 30 µg/ml of Topiramate. All dilutions were scanned at specific wavelength against methanol as blank. The spectrum of the drug was studied to verify λmax and calibration curve was plotted with absorbance verses concentration.

Drug and polymer compatibility study

Fourier transform infrared spectroscopy

The study was conducted with an intension to check the compatibility of natural polymer i.e. chitosan, pectin with Topiramate. Also, it helps to check the suitability of polymers for the preparation of nanoparticle. FTIR spectrum was studied using a Shimadzu FTIR spectrometer. The samples of pure drug and physical mixture such as Topiramate with chitosan and pectin were prepared separately with KBr after drying in hot air oven for about 1 hr then kept in desiccators before scanning the spectra between the ranges of 4000 to 500 cm^{-1}.

Differential scanning calorimetry

The thermal behavior of pure drug, chitosan/pectin and drug loaded chitosan pectin nanoparticles was carried out using differential scanning calorimeter (Meter Toledo) at a heating rate of 10℃/min. The measurements were performed at a heating range of 30 - 400℃ under nitrogen atmospheres.

Preparation of Topiramate Loaded Chitosan based Polyelectrolyte Complex

Ionic gelation method was used to create topiramate-loaded CS-based PEC. According to Table 1, typical amounts of chitosan were largely dissolved in various ratios of aqueous acetic acid. To prepare a Pectin solution of various strengths with deionized water, 1 mg of Topiramate was added. Then, while constantly stirring, 10 ml of the Topiramate-Pectin solution was added drop by drop to 10 ml of the CS solution. For 30 minutes, the mixture was agitated at room temperature to obtain loaded PEC. Additionally, PEC that had spontaneously formed were separated by centrifugation for 10 minutes at 4750 rpm, with the supernatant being discarded [23,24].

Table 1: Formulation parameters for Topiramate loaded chitosan-based PEC- 3^3 factorial design

Independent Variables	Levels			Dependent Variables	Constraints
	-1	1	+1		
Concentration of Chitosan (% w/v)	0.1	0.2	0.3	Particle Size	Minimum
Concentration of Pectin (% w/v)	0.25	0.5	0.75	EE	Maximum
Concentration of AA (% v/v)	0.5	0.75	1.0	-	-

Factorial design and optimization

For optimisation, the current study used three full-level factorial designs (33: add up to 32 runs). Stat-Ease Inc., Minneapolis, USA, provided DESIGN EXPERT 8.0 for use in the statistical experimental design. In order to evaluate the factor relationship between the variables, response surface graphs were employed. The concentration of CS (X_1), Pectin (X_2), and AA (X_3) were three of the independent variables that were taken into consideration. The three factorial levels for these variables are coded as 1, 0 and +1 for low, medium, and high levels, respectively. As dependent variables, particle size (PS-Y_1) and entrapment effectiveness (EE-Y_2) were used.

For the purpose of studying and optimising the interaction between each level and the formulation characters, a total of 32 trial runs (along with five centre point batches) were required. The statistical validity of the produced polynomial equations was established using ANOVA. All the observed responses were simultaneously fitted to various models. In order to determine the statistically best-fitting experimental model (main, interaction, and quadratic), numerous statistical metrics were compared, including the CV (coefficient of variation), R^2 (multiple correlation coefficient), adjusted R^2 (Adju.R^2), and projected R^2 (Pred.R^2). The threshold for significance was set at $p < 0.05$. To determine the response (Yi) in each trail, multiple factorial regression analysis (2FI for particle size and quadratic model for EE) was used [25,26].

$Yi(2FI) = b_0 + b_1X_1 + b_2X_2 + b_3X_3 + b_4X_1X_2 + b_5X_1X_3 + b_6X_2X_3$

$Yi\ (Quadratic) = b0 + b_1X_1 + b_2X_2 + b_3X_3 + b_4X_1X_2 + b_5X_1X_3 + b_6X_2X_3 + b_7X^2_1 + b_8X_2^2 + b_9X^2_3$

where

Y_i – Dependent variable;

b_0 – Arithmetic mean response of all trials;

b_i – the Estimated coefficient for factor Xi,

X_1, X_2, and X_3 (Main effects) – Average value of changing factor one at a time

X_1X_2 and X_1X_3 and X_2X_3 – Represent the interaction terms and

X_1^2 , X_2^2 and X_3^2 – The polynomial terms

Characterization of Topiramate loaded CS based PEC

Determination of particle size (PS)

Zetasizer (Malvern Master Sizer 2000, UK) was used to measure the particle size (Z-average mean) of prepared topiramate-loaded chitosan-based PEC. Three measurements were made for each measurement [27].

Entrapment efficacy (EE)

EE is the ratio of the real theoretical amount of drug to the practical amount of drug trapped in the polymer. The supernatant from the centrifuged nanosuspension of topiramate-loaded chitosan-based PEC was then tested for free topiramate by measuring the absorbance at 272 nm (REMI centrifuge, C-24 BL, India). By changing the total and free amounts of topiramate in the formula below, EE was computed [28].

$$EE\ \% = \frac{\text{Topiramate } X_T - \text{Topiramate } X_F}{\text{Topiramate } X_T} \times 100$$

where Topiramate X_T = total amount of topiramate used in the preparation of PEC and Topiramate X_F = free topiramate present in the supernatant.

Preparation of checkpoint batch for validation of experimental design

An optimised batch of PEC (OPEC-1) was created using optimised concentrations of CS, Pectin, and AA and tested for use in EE, PS, PDI, morphological evaluation, and in vitro drug release investigations [29]. The following Eq. (1) was used to calculate relative error in order to validate the experimental design.

$$\text{Relative error } \% = \frac{\text{Predicted Value} - \text{Practical Value}}{\text{Predicted Value}} \times 100$$

Scanning electron microscopy (SEM)

PEC coated with a thin gold palladium layer by sputter coater unit (VG – Microtech, United Kingdom) and the surface topography was analyzed with a Cambridge stereoscan S120 SEM operated at an acceleration voltage of 10 KV [30].

Transmission electron microscopy

The morphology of optimized PEC-1 was observed using TEM. The powder of PEC was placed on a carbon-coated copper grid and negatively stained with 2% (w/v) phosphotungstic acid solution. The grid was allowed to dry at room temperature. The stained film placed on a holder was viewed under TEM operated an accelerating voltage of 80 KV.

X-ray diffraction analysis

The Philips PW 1729 X-ray diffractometer was used to investigate the XRD of pure drug and optimized batch of PEC. Samples were exposed to monochromatized Cu K-radiations (1.542 A°), and they were then examined between 2 and 60 degrees. 30 kV and 30 mA were the employed voltage and current, respectively. The chart speed was kept at 100 mm/2 and the range was 5 103 cycles/s.

In-vitro drug release study

PBS (pH 7.4) was used to carry out drug release evaluation from OPEC-1 for roughly 18 hours. A dialysis bag was used to hold an aliquot of OPEC-1 that had been pre-mixed with topiramate and suspended in 50 ml of phosphate buffered solution (PBS) at 37 °C with moderate magnetic stirring (100 rpm). To keep the sink conditions constant, 3 ml of sample was taken out and replaced with an equal volume of fresh medium at various time intervals. To measure the amount of topiramate

released, samples were examined using a UV visible spectrophotometer (Shimadzu UV-1700, China) at a predetermined wavelength of 272 nm [31].

Ex-vivo permeation studies

The optimised batch's ex-vivo permeation investigation was carried out utilising freshly excised sheep nasal mucosa, which was procured from the nearby abattoir within an hour of the animal being sacrificed, as the bio membrane. With the mucosal and serosal surfaces pointing towards the donor and receptor compartments, respectively, nasal mucosa was carefully sliced and installed on the diffusion chamber. The Franz diffusion cell, which has a receptor capacity of 12.0 ml and a permeation area of 3.14 cm2, was used to assess the drug diffusion characteristic. The pH 6.6 phosphate buffers in the receptor phase were kept at 371 °C throughout the course of the experiment by constant stirring. The donor compartment received PEC that was equal to 10 mg of topiramate. To keep the sink conditions constant, 300 ± l of the sample was taken out of the receiver compartment at regular intervals and replaced with an equal volume of new buffer solution. Each experiment was carried out in triplicate, and the sample was evaluated spectrophotometrically at a wavelength of 272 nm using phosphate buffer (pH 6.6) as a blank [32].

Ex-vivo biocompatibility studies

To ascertain whether prepared PEC is biocompatible with nasal mucosa. Freshly removed sheep nasal mucosa that had been carefully washed with isotonic saline solution was used for the histology analysis. On the nasal mucosa, prepared topiramate PEC (100 mg) was placed correctly. It was routinely treated, embedded in paraffin, and preserved in 10 % neutral carbonate buffered formalin solution after one hour. To ensure the tissue's viability, the experiment was conducted in a cell culture incubator (Sanyo Incubator, Model MCO-5AC, and Japan). Haematoxylin-Eosin (HE) indicator was used to stain additional paraffin sections (7.5 m), which were then examined under a Motic microscope. After isolation, the untreated mucosa that was directly glued was used as a control [33].

Result and Discussion

Ultraviolet – visible spectroscopy

a) Determination of λmax

An absorption maximum was found to be at 272 nm. Hence 272 nm was selected as λ max for further studies.

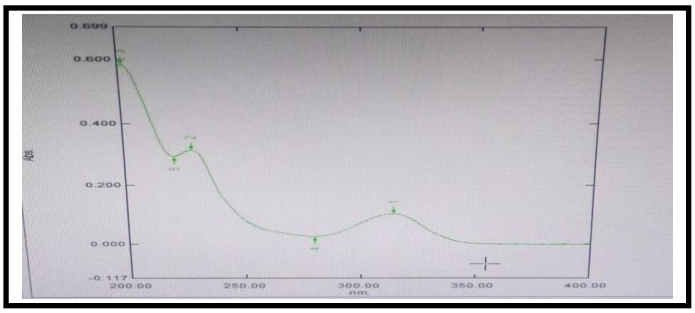

Fig. UV Spectrum of Topiramate

An absorption maximum was found to be at 272 nm. Hence 272 nm was selected as λ max for further studies

b) Calibration curve of Topiramate

The stock solution for the standard drug of 1 mg was prepared using 100 ml of water. The maximum absorbance for the drug solution of 10 mcg/ml was found to be at 272 nm. The linearity was found between the concentration range of 10-35 mcg/ml for UV spectroscopy**.**

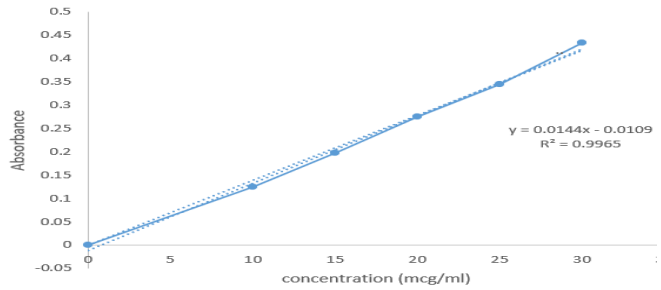

Fig. Calibration curve of Topiramate in water

Drug–excipient interactions study

Fourier-transform infrared spectroscopy (FTIR)

FTIR spectrum of Topiramate was shown in following Fig. revealed characteristic peaks representing the presence of functional groups claim by its chemical structure. From this we can consider that the Topiramate was of pure quality.

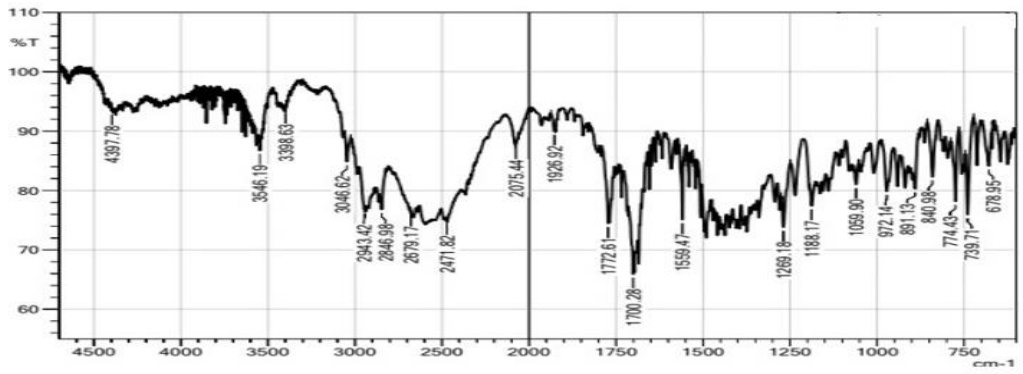

Fig. FTIR spectra of Topiramate

After interpretation of FT-IR Spectrum of drug, it was concluded that all the characteristic peaks corresponding to the functional group present in the molecular structure of Topiramate were found within the reference range and confirming its identity.

Table: Drug Interpretation data of FTIR

Material	**Functional group**	**Standard IR ranges (cm-)**	**Observed IR ranges (cm-)**
Topiramate	C -O stretching N-H stretching	1720-1850 1500-1600	1772.61 1559.47

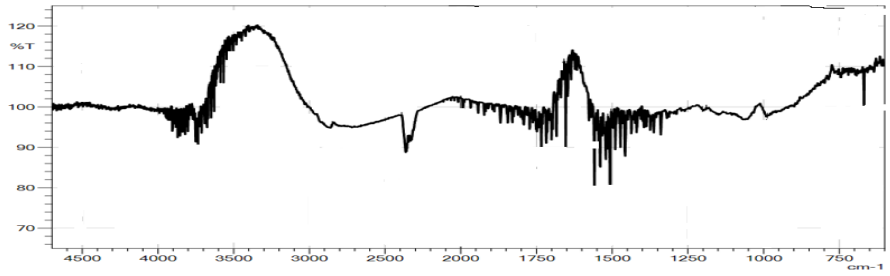

Fig. FTIR Spectra of Chitosan

After interpretation of FT-IR Spectrum of polymer, it was concluded that all the characteristic peaks corresponding to the functional group present in molecular structure of chitosan were found within the reference range, confirming its identity.

Table: Polymer Interpretation data of FTIR

Material	**Functional group**	**Standard IR Ranges (cm^{-1})**	**Observed IR Ranges (cm^{-1})**
Chitosan	O-H Stretching C-O Stretching C=O Stretching	3300-2500 1382-1036 1680-1630	2857.87 1199.56 1654.23

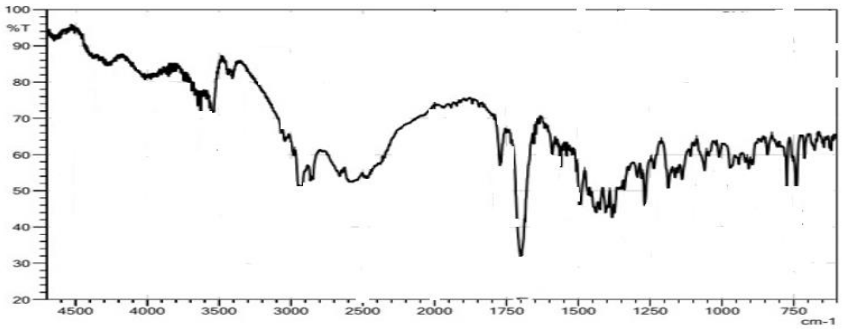

Fig. FTIR Spectra of Physical Mixture

After interpretation of FT-IR Spectrum of Chitosan and its physical mixture with drug, it was concluded that all the characteristic peaks corresponding to the functional group present in molecular structure of Topiramate were not found intact within the reference range, confirming its reactivity with chitosan. This interaction further supports the selection of polymer.

Table: Physical mixture Interpretation data of FTIR

Material	**Functional group**	**Standard IR Ranges (cm^{-1})**	**Observed IR Ranges (cm^{-1})**
Physical mixture (Topiramate + Chitosan + Pectin)	C-N Stretching C-H Stretching O-H Stretching	1350 – 1250 2850 – 2970 3650 - 3450	1268.22 2946.32 3558.73

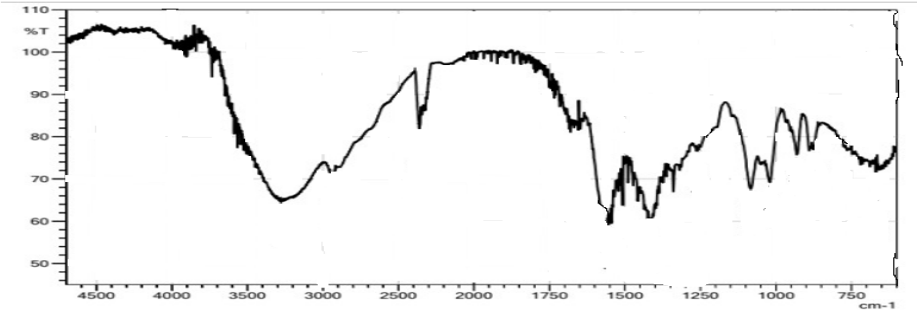

Fig. FTIR Spectra of Formulation OPEC-1

Table: Formulation Interpretation data of FTIR

Material	**Functional group**	**Standard IR Ranges (cm^{-1})**	**Observed IR Ranges (cm^{-1})**
Formulation	C – H Stretching C- N stretching	2850 – 2970 1350 – 1250 1200 – 1000	2938.65 1261.55 1085.97

There was no considerable change in the positions of characteristic absorption bands and bonds of various functional groups present in the drug. This observation clearly suggests

that the Topiramate shows no prominent change in its characteristics even in its physical mixture. The results of FTIR spectra indicated the interaction between drug and polymer. It showed that Topiramate was compatible with chitosan.

Preparation and optimization of PEC

Design expert software projected 32 experimental runs from the three complete level factorial design for the three components of Chitosan (CS) (X_1), Pectin (X_2), and Acetic acid (AA) (X_3), which were adjusted at three distinct levels (coded as 1, 0 and +1). For this investigation, the response parameters of particle size (PS-Y1) and entrapment efficacy (EE-Y_2) were examined. Table 2 displayed a thorough outline of three full-level factorial designs.

Table 2: Experimental runs for 3 full level factorial design

Conc. of CS (X1)	Conc. of Pectin (X2)	Conc. of AA (X3)	PS (Y1)	EE (Y2)
0.10	0.10	0.50	513	59
0.10	0.15	0.50	488	70
0.10	0.20	0.50	421	76
0.10	0.10	0.75	519	71
0.10	0.15	0.75	421	80
0.10	0.20	0.75	399	69
0.10	0.10	1.00	481	77
0.10	0.15	1.00	390	81
0.10	0.20	1.00	321	65
0.20	0.10	0.50	376	75
0.20	0.15	0.50	355	81
0.20	0.20	0.50	322	67
0.20	0.10	0.75	369	80
0.20	0.15	0.75	343	83
0.20	0.20	0.75	302	70
0.20	0.10	1.00	399	79
0.20	0.15	1.00	355	85
0.20	0.20	1.00	300	78
0.20	0.15	0.75	346	77
0.20	0.15	0.75	341	80
0.20	0.15	0.75	343	80
0.20	0.15	0.75	347	77
0.20	0.15	0.75	349	70
0.30	0.10	0.50	302	81
0.30	0.15	0.50	288	84
0.30	0.20	0.50	265	75
0.30	0.10	0.75	289	86
0.30	0.15	0.75	255	90
0.30	0.20	0.75	220	76
0.30	0.10	1.00	275	76
0.30	0.15	1.00	224	84
0.30	0.20	1.00	202	88

For 3^2 batches, the PS and EE values varied from 202 nm to 519 nm and 59% to 90%, respectively. To determine the quantitative effects of the fact factors, an ANOVA was conducted. Multiple regression was used on the data to produce polynomial equations (2FI model for PS and quadratic model for EE). Model terms are considered significant when their values are $p < 0.05$. While a negative sign denotes an antagonistic or inverse influence of the component on the chosen response, a positive number denotes a synergistic interaction that Favours optimisation. Below are the residual equations for two dependent variables expressed in terms of coded components.

Particle size = $+ 347.51 - 91.73X_1 - 43.84X_2 - 22.29X_3 + 17.09X_1X_2 + 7.34X_1X_3 - 13.43X_2X_3$

EE = $+ 77.47 + 4.78X1 + 7.33X2 + 2.67X3 - 0.25X1X2 - 0.75X1X3 - 0.67X2X3 + 0.70X^2_1 - 2.30X^2_2 - 1.30X^2_3$

While the quadratic model with an R^2 value of 0.9817 was recommended for the EE response, the 2FI model for PS was found to have a significant R^2 value of 0.9754. High values of Adju. R^2 (Adjusted coefficient of determination) (Table 3) further demonstrate that all models for both responses match experimental data well.

Table 3: Model statistical summary

Response	Models	R^2	Adju.R^2	Pred. R^2	Adequate precision	S.D	Remarks
P.S	Linear	0.9484	0.9418	0.9232	-	22.09	Suggested
	2 FI	0.9754	0.9670	0.9511	40.554	17.75	
	Quadratic	0.9759	0.9619	0.9317	-	18.72	
	Cubic	0.9916	0.9924	0.9561	-	11.73	Aliased
E.E	Linear	0.9367	0.9289	0.9246	-	3.07	
	2 FI	0.9446	0.9289	0.8953	-	3.07	
	Quadratic	0.9817	0.9700	0.9517	37.543	2.46	Suggested
	Cubic	0.9684	0.9798	0.9487	-	2.27	

Also discovered to be in fair agreement with Adju.R^2 (0.9670 for PS and 0.9700 for EE) values were Pred. R^2 values (0.9511 for PS and 0.9517 for EE). Additionally, 'Adequate accuracy' is generally used to evaluate the signal-to-noise ratio (predicted response relative to its associated error), and a ratio of larger than four is typically preferred for navigating the design space. The signal to noise ratios for PS and EE were 40.554 and 37.543, respectively, demonstrating the good suitability of the chosen model. When the results were shown graphically for both investigated reactions, the experimental data acquired demonstrated a strong correlation with the expected data. The natural logarithm of the sum of the squares or residuals is typically used as a guideline for choosing the precise power law transformation (lambda), which is established at the minimum point of the curve. To achieve the best fitting models, recommended transformations were put forth based on the best lambda values. Thus, for two suggested models, 2FI(PS) and quadratic models (EE), the suggested powers as a result of the best lambda were 0.62 and 0.18, respectively.

The non-significant lack of fit ($p<0.05$ of the 5% significant level) obtained from all the models can be used to confirm that the data fit the suggested models. Indicating the model is significant, the model F-values of 116.55 for PS (2FI) and 84.61 for EE (quadratic) indicate that there is only a 0.01% probability that a model F-value may result from noise. Both F and p values were used to assess the relevance of the model's coefficients based on the ANOVA findings (Table 4).

Table 4: Analysis of variance (ANOVA) results

Term	**Responses**					
	PS			**EE**		
	Coefficients	**F-Value**	**p value**	**Coefficients**	**F-Value**	**p value**
X_1	-91.73	529.72	<0.0001	5.79	196.68	<0.0001
X_2	-43.84	118.87	<0.0001	8.34	461.99	<0.0001
X_3	-22.29	30.09	<0.0001	3.68	61.97	<0.0001
$X_1 X_2$	17.09	12.09	0.0028	-0.26	0.37	0.5663
$X_2 X_3$	7.34	2.73	0.2120	- 0.76	4.22	0.0969
$X_1 X_3$	-13.43	7.61	0.0166	-0.68	3.54	0.1354
X^2_1	-	-	-	0.71	2.70	0.2172
X^2_2	-	-	-	- 3.31	18.96	0.0004
X^2_3	-	-	-	-2.31	6.73	0.0259

Response Y1 (PS) was significantly influenced by i) antagonistic effect of X1, X2 and X3 (all with a probability value of <0.001) and X1X2 (p-value 0.0028); ii) synergistic effect of X2X3 with a p value of 0.0166, being X1 effect the highest. Response Y2 (EE) was significantly influenced by i) synergistic effect of X1, X2 and X3 (all with a probability value of <0.001); ii) antagonistic effect of polynomial terms of X2 and X3 (X^2_2 , X_3^2) with a p-value of 0.0004 and 0.0259 respectively. Among all these significant variables, X2 effects EE with more magnitude. Response surface methodology (RSM) was used to further explain and examine the influence of independent variables on replies. RSM allows for the learning of primary effects and interaction effects with three-dimensional response surface graphs (RSG). Visual representations of measured responses are provided by contour plots. According to the RSG and parallel contour plots (Fig. 1) relating PS, the reaction declines as X_1X_2, X_1X_3, and X_2X_3 concentrations rise. Fig. 2's contour and 3-D response surface plots show that when EE increased, all variable concentrations also increased.

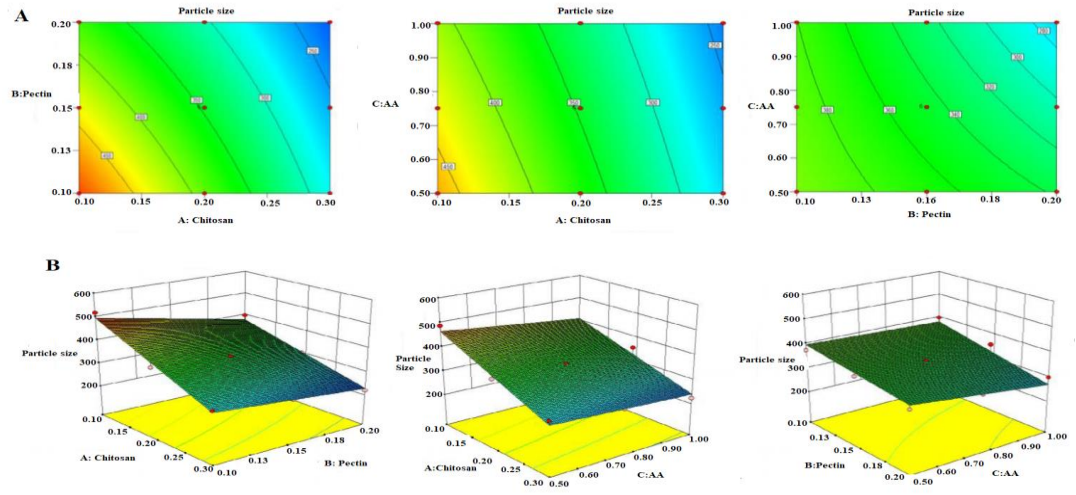

Fig. 1. Contour plots (A) and three-dimensional response surface plots (B) for PS (Y1)

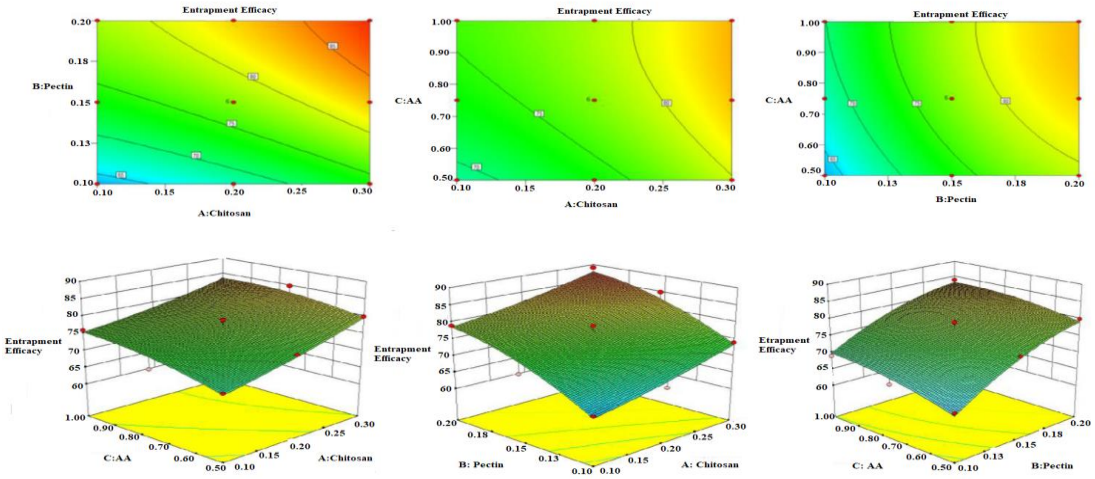

Fig. 2. Contour plots (A) and three-dimensional response surface plots (B) for EE (Y2)

Setting objectives for each response and then making an overlay graph allowed for the independent variables to be optimised. To simultaneously optimise the sequence of models derived from experimental statistical analysis, the global desirability function (D) was used. At their design space, the optimisation considered all three independent factors. Each response has a low and high value given to each target for concurrent optimisation. While EE adjusted maximise, the PS reaction was set to a minimal target. As a result, for each response, whose values were stated using a non-dimensional scale ranging from 0 to 1, a unique desire function (D) was provided. Desirability plots display areas of various hues that express D's range. Dark blue represents the least desirable zone with a D value close to zero, while red represents the most desirable zone with a D value of 1. D values between 0 and 1 were indicated by additional coloured zones. The maximum D value of 0.979 for both replies' desirability plots was attained at ideal independent variable concentrations. The usage of such conditions will therefore result in modest PS (202 nm) and maximal EE (90.4%). As a result, the ideal concentrations of independent variables were taken into consideration when creating OPEC-1.

Evaluation of checkpoint batch (OPEC-1)

Formulation (OPEC-1) was produced and assessed for EE, PS, PDI, morphological evaluation, and in vitro drug release experiments utilising optimised concentrations. By contrasting actual and expected values, the experimental design was quantitatively validated. Both responses' relative errors (%) were calculated, and the results were judged to be within an acceptable range of + 5%. The experimental outcomes and expected results were comparatively similar, demonstrating how precisely the design was done.

PDI and zeta potential

It is commendable to point out that OPEC-1 was distinguished by a limited PS distribution, as shown by the PDI value of 0.219 + 0.0313, X1 displays the synergistic effect on PDI, and furthermore, greater EE equals less PDI, which indicates a homogenous PEC system. In order to produce stable nano dispersions, OPEC-1 demonstrated a positive surface charge that is significant enough to demonstrate electrostatic repulsions between produced PEC. The total number of free -NH3+ chitosan molecules that are present on the PEC surface is determined by the strength of the positive charge. The information on the electrostatic potential and colloidal stability of the particles in solution is given by the quantifiable measure known as zeta potential. A high voltage of (>30 mV and 30 mV) is thought to be beneficial for prepared dispersions' strong stability. It was discovered that OPEC-1 has a zeta potential of 30.8 0.75 mV, which guarantees the great stability of prepared PEC.

Scanning Electron Microscopy (SEM)

Scanning electron microscopy was done for the surface characterization of OPEC-1 formulation. As shown in fig. the OPEC-1 Formulation was scanned on 5,000x, 15,000x and 3000x.

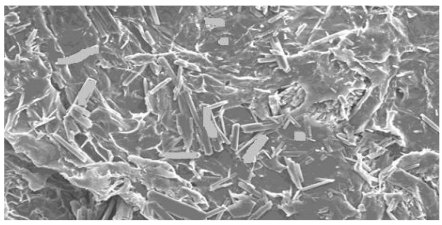

Fig. 3: SEM image of the chitosan based Topiramate OPEC-1

It does not show spherical structure. It shows irregular structure.

Transmission electron microscopy

Size and shape of the optimized batch of PEC were evaluated by transmission electron microscopy (TEM). TEM images of the PECs nanoparticle confirmed spherical shape of nanoparticles with narrow size distribution and non- aggregation and clumping of nanoparticles.

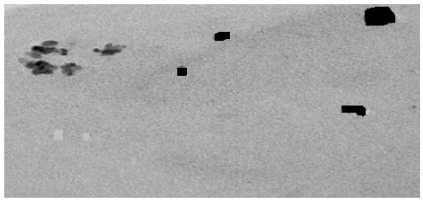

Fig. 4: TEM image of chitosan based Topiramate OPEC-1

Differential scanning colorimetry

The DSC thermogram of Topiramate, Chitosan, Pectin, and OPEC-1 are shown in figure.

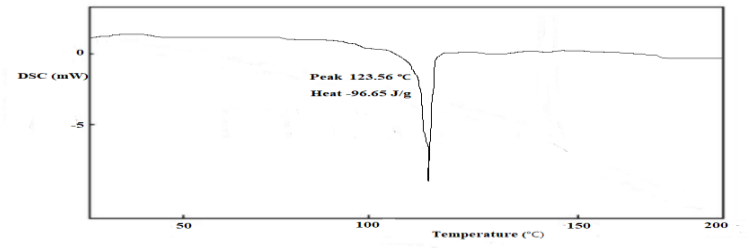

Fig. 5: DSC Thermogram of Topiramate

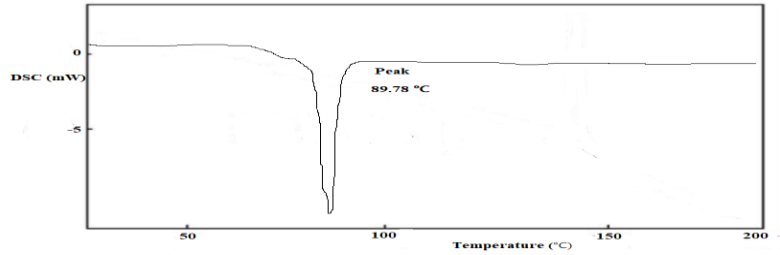

Fig. 6: DSC thermogram of Chitosan

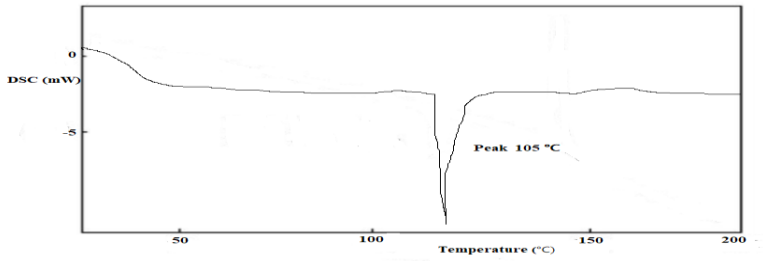

Fig. 7: DSC thermogram of pectin

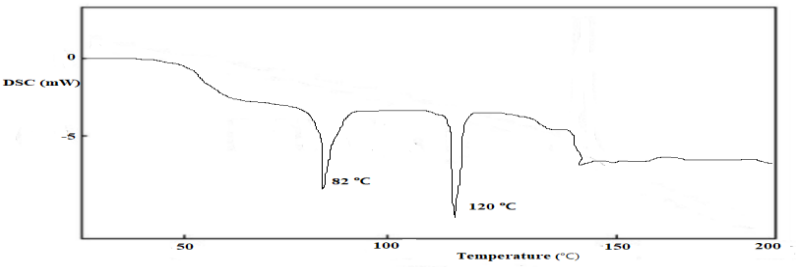

Fig. 8: DSC thermogram of OPEC-1

The thermal analysis of pure drug, chitosan, pectin and OPEC-1 formulation were studied by using Differential Scanning Calorimetry (DSC) as shown in following fig. respectively. The Topiramate shows endothermic peak at approximately 123.56 °C. Chitosan shows a sharp endothermic peak at 89.78 °C corresponding to its melting point. The Pectin showed endothermic peaks at 105°C respectively. DSC thermogram of drug loaded PEC chitosan nanoparticles (OPEC-1) shows the two endothermic peaks at 82°C and 120 °C.

X-ray diffraction study (XRD)

The X-ray diffraction pattern of pure drug Topiramate, chitosan-based OPEC-1, and both polymer i.e., chitosan and Pectin were recorded on an x-ray diffractometer shown in fig. The distinctive sharp peaks of drug were observed at diffraction angles, 11.657 º, 12.852 º, 18.234 º on 2ɵ scale, illustrating the typical crystalline nature of drug. The nanoparticles showed a broad peak 22.267 º for indicating the amorphous state of the polymer. The absence of crystalline peaks of Topiramate in drug loaded PEC confirmed that the drug was molecularly dispersed in the polymer and conversion of drug into the amorphous form takes place.

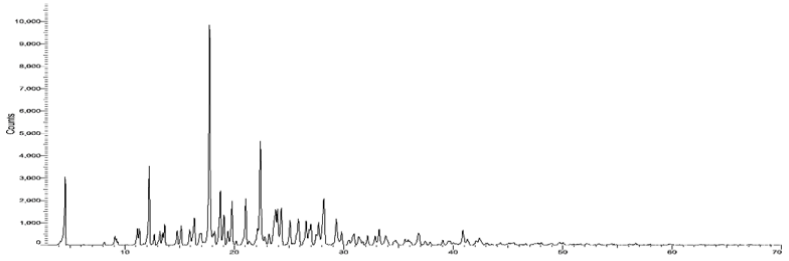

Fig. 9: XRD of pure drug Topiramate

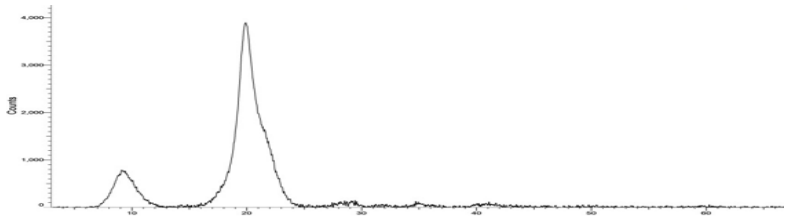

Fig. 10: XRD of Chitosan

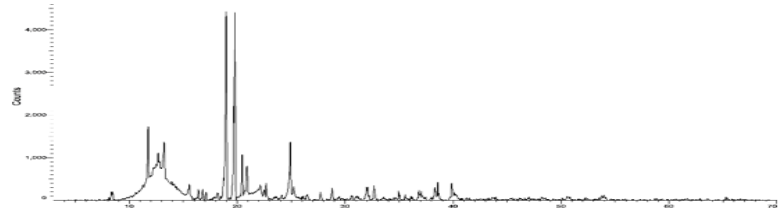

Fig.11: XRD of Pectin

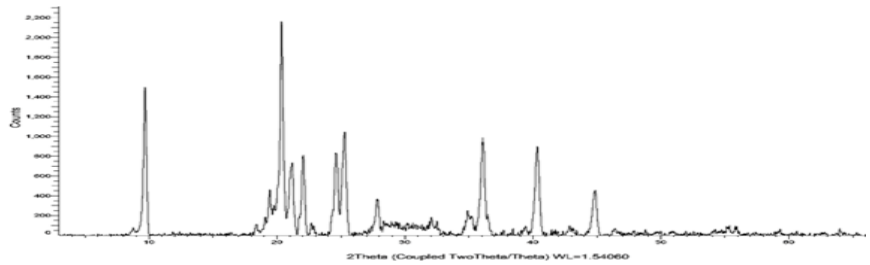

Fig. 12: XRD of drug loaded chitosan-based OPEC-1

In-vitro drug release

Studies on OPEC-1's in-vitro drug release revealed that 25.26% of the drug was released in a burst shortly after one hour, whereas 90.5% of the drug was released after 18 hours. This was consistent with the controlled drug release of topiramate from prepared PEC. The initial burst release of 25.26% from the PEC formulation within 1 hour was consistent with in vitro dissolution data, which were then followed by prolonged controlled drug release. On the PEC surface, where the drug molecules are loosely integrated by weaker electrostatic contact between the positive charged amino group of chitosan, the initial quick release of topiramate may be recognized as part of the substance. Fig. 13 displays comparative dissolution characteristics of pure topiramate and an improved formulation.

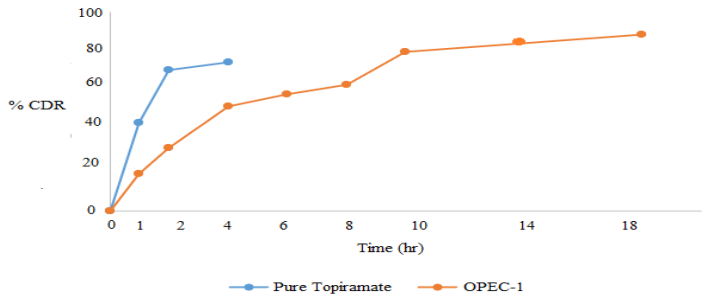

Fig.13: In vitro release pattern of OPEC-1

Ex-vivo permeation studies

The optimised formulation OPEC-1 underwent the ex-vivo permeation investigation. After 180 minutes, it was discovered that 90.04% of the topiramate had permeated from the PEC of batch OPEC-1, as shown in fig. 14. Chitosan, a cationic bio adhesive polymeric substance, can be used to improve medication absorption and dissolution when incorporated in PEC formulations for intranasal administration. The increased surface area provided by the smaller PEC particle size increases the drug release from formulations.

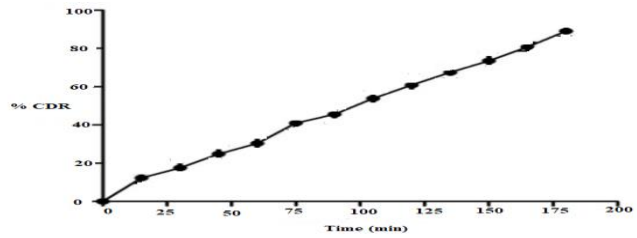

Fig. 14: Ex-vivo permeation of topiramate loaded chitosan-based PEC of OPEC-1

Ex-vivo biocompatibility studies

When preparing nasal PEC, it is crucial to protect the integrity of the nasal mucosa because prolonged exposure can compromise the nasal membrane's safety. The nasal mucosa treated with PEC and medication did not exhibit any deformation. The produced formulation is safe and biocompatible for intranasal administration, according to the findings of biocompatibility experiments.

A) **B)**

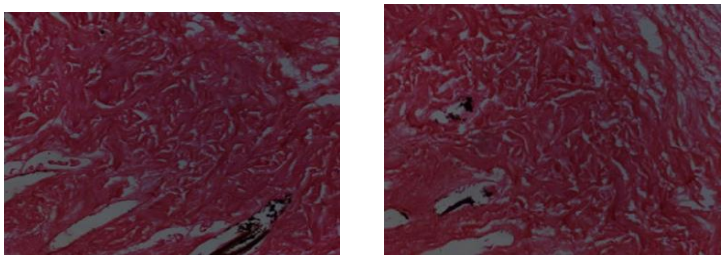

Fig. 15: H**istopathological specimen of A) untreated nasal mucosa, B) topiramate loaded chitosan-based PEC treated nasal mucosa**

Conclusion

The current work proved that chitosan-based PEC of topiramate may be successfully formulated using the ionotropic gelation process. Percentage yield, entrapment effectiveness, bioadhesion potential, ex vivo biocompatibility, and an in vitro drug diffusion profile analysis were used to describe the formulation. The findings of the topiramate-loaded PEC biocompatibility study showed that chitosan is a safe and biocompatible polymer that may be placed to the nasal epithelium, increasing the drug's absorption and bioavailability. Therefore, when compared to its traditional mode of administration and dose type, topiramate PEC delivery via intranasal inhalation is the better option.

References

1. Gautam S., Nikalaje Y., Bhadre D., Trivedi R., Umekar M., Taksande J. Development and evaluation of lamotrigine soya lecithin solid dispersion: *in vitro* and pharmacodynamic investigation**.** Int J Appl Pharm. 2019;12:115-22.
2. Musumeci T., Bonaccorso A., Puglisi G. Epilepsy disease and nose-to-brain delivery of polymeric nanoparticles: an overview. Pharmaceutics. 2019;11:118.
3. Fisher RS., Ho J. Potential new methods for antiepileptic drug delivery. CNS Drugs. 2002;16:579-93.
4. Bhuva F., Patel LD., Patel K. Factorial design methodology for development of pediatric nasal spray: study on xylometazoline nasal solution used for treatment of nasal congestion. Indian J Pharm Edu Res. 2018;52:218-29.
5. Mantry S., Balaji A. Formulation design and characterization of ropinirole hydrochloride microsphere for intranasal delivery. Asian J Pharm Clin Res. 2017;10:195-203.
6. Lopez T., Cuevas JL., Jardon G., Gomez E., Ramirez P. Preparation and characterization of antiepileptic drugs encapsulated in sol-gel titania nanoparticles as controlled release system. Med Chem. 2015; 2:3.
7. Tas C., Ozkan CK., Savaser A., Ozkan Y., Tasdemir U., Altunay H. Nasal administration of metoclopramide from different dosage forms: *in vitro*, ex vivo, and *in vivo* evaluation. Drug Delivery. 2009;16:167-75.
8. Dhanda DS., Frey WH., Leopold D., Kompella UB. Approaches for drug deposition in the human olfactory epithelium. Drug Delivery Technol. 2005;5:64-72.
9. Gavini E., Rassu G., Sanna V., Cossu M., Giunchedi P. Mucoadhesive microspheres for nasal administration of an antiemetic drug, metoclopramide: *in-vitro/ex-vivo* studies. J Pharm Pharmacol. 2005;57:287-94.
10. Al-Nemrawi NK., Alsharif SS., Dave RH. Preparation of chitosan-TPP nanoparticles: the influence of chitosan polymeric properties and formulation variables. Int J Appl Pharm. 2018;10:60-5.

11. Hagesaether E. Permeation modulating properties of natural polymers–effect of molecular weight and mucus. Int J Pharm. 2011;409:150-5.
12. Soni M., Majumdar A., Malviya N. Mucoadhesive chitosan microspheres of gefitinib. Int J Curr Pharm Res. 2018;10:9-19.
13. Santos Magalhaes NS., Pontes A., Pereira VM., Caetano MN. Colloidal carriers for benzathine penicillin G: nanoemulsion and nanocapsules. Int J Pharm. 2000;208:71-80.
14. Kulkarni A., Bambole VA., Mahanwar PA. Electrospinning of polymers, their modelling and applications. Polymer Plastics Tech Eng. 2010;49:427-41.
15. Taksande JB., Sonwane PP., Trivedi RV., Wadher KJ., Umekar MJ. Formulation and pharmacodynamic investigations of lamotrigine microspheres in pentylenetetrazole-induced seizures in mice. Asian J Pharm. 2017;11:S216-24.
16. Taksande JB., Umekar MJ. Preparation of intranasal pregabalin microspheres: *in vitro*, ex vivo and *in vivo* pharmacodynamic evaluation. J Pharm Res. 2018;12:112-21.
17. El-din EY., Omar AR. Effect of prenatal administration of therapeutic dose of topiramate on placentae albino rats' fetuses. Int J Pharm Sci. 2017;9:54-9.
18. Sommer BR., Mitchell EL., Wroolie TE. Topiramate: effects on cognition in patients with epilepsy, migraine headache and obesity. Ther Adv Neurol Disord. 2013;6:211-27.
19. Doose DR., Walker SA., Gisclon LG., Nayak RK. Single-dose pharmacokinetics and effect of food on the bioavailability of topiramate, a novel antiepileptic drug. J Clin Pharmacol. 1996;36:884-91.
20. Britzi M., Soback S., Isoherranen N., Rene H L., Perucca E. Analysis of topiramate and its metabolites in plasma and urine of healthy subjects and patients with epilepsy by use of a novel liquid chromatography-mass spectrometry assay. Ther Drug Monit. 2003;25:314-22.
21. L.P. Chandrika, S. Fereidoon. Optimization of extraction of phenolic compounds from wheat using response surface methodology. Food Chem. 2005; 93(1): 47–56.
22. N. Hatambeygi, G. Abedz, M. Talebi. Method development and validation for optimized separation of salicylic, acetyl salicylic and ascorbic acid in pharmaceutical formulations by hydrophilic interaction chromatography and response surface methodology, J. Chromatogr. A. 2011; 1218 (35): 5995–6003.
23. S. Vimal., G. Taju., K.S.N. Nambi, S. Abdul-Majeed, V. Sarath Babu, M. Ravi, A.S. Sahull Hameed. Synthesis and characterization of CS/TPP nanoparticles for oral delivery of gene in fish. Aquaculture. 2012; 56: 358–359.
24. E. Gundogdu, I.O. Derya, E. Meliha, O. Emre, A. Makbule. Radiolabeling efficiency and cell incorporation of chitosan nanoparticles. J. Drug Deliv. Sci. Tec. 2015; 29: 84–89.
25. A.K. Nayak, D. Pal, K. Santra. Development of calcium pectinate-tamarind seed polysaccharide mucoadhesive beads containing metformin HCl. Carbohydr. Polym. 2014; 101: 220–230.
26. J. Malakar, A.K. Nayak. Formulation and statistical optimization of multiple unit ibuprofen-loaded buoyant system using 23 -factorial design. Chem. Eng. Res. Des.2012; 11: 1834–1846.
27. S. Rimple, A. Munish, K. Harmanmeet, Thiolated pectin nanoparticles: preparation, characterization and ex vivo corneal permeation study. Carbohydr. Polym. 2012; 87 (2): 1606–1610.
28. Munish A Shelly, K. Ashok. Gum ghatti–chitosan polyelectrolyte nanoparticles: preparation and characterization, Int. J. Biol. Macromolec. 2013; 61: 411–415.
29. Z. Karami, M.R. Saghatchi Zanjani, N. Nasihatsheno, M. Hamidi. Improved oral bioavailability of repaglinide, a typical BCS Class II drug, with a chitosan coated nanoemulsion. J. Biomed. Mater. Res. 2019; 54: 1–12.
30. Jingou Ji, Wu. Danjun, Li Liu, Jida Chen, Xu. Yi. Preparation evaluation, and In vitro release of folic acid conjugated O-Carboxymethyl chitosan nanoparticles loaded with methotrexate. J. Appl. Polym. Sci. 2012; 125: E208–E215.

31. D.R. Nogueira, L. Tavano, M. Mitjans, L. Perez, M.R. Infante, M.P. Vinardell. In vitro antitumor activity of methotrexate via pH-sensitive chitosan nanoparticles. Biomaterials. 2013; 34:2758–2772.
32. Chalikwar SS., Mene BS, Pardeshi CV., Belgamwar VS., Surana SJ. Self-assembled, chitosan grafted PLGA nanoparticles for intranasal delivery: design, development and ex vivo characterization. Polymer Plastics Technol Eng 2013;52:368-80.
33. Pardeshi CV., Belgamwar VS. Controlled synthesis of N, N, N-trimethyl chitosan for modulated bio adhesion and nasal membrane permeability. Int J Bio Macromol. 2016;82:933-44.
34. SL Patwekar, MK Baramade. Controlled release approach to novel multiparticulate drug delivery system. Int J Pharm Pharm Sci 4 (3), 757-63
35. SL Patwekar, AB Suryawanshi, MS Gaikwad, SR Pedewad, AP Potulwar. Standardization of herbal drugs: An overview. The Pharma Innovation 5 (4, Part B), 100.
36. SL Patwekar, SG Gattani, MM Pande. Needle free injection system: A review. Int J Pharm Pharm Sci 5 (4), 14-19.
37. JDS Khayyam Shaikh , Shailesh Patwekar , Santosh Payghan. Dissolution and Stability Enhancement of Poorly Water Soluble Drug – Lovastatin by Preparing Solid Dispersions. Asian Journal of Biomedical and Pharmaceutical Sciences 1 (4), 24-31
38. PG Jamkhande, VA Suryawanshi, TM Kaylankar, SL Patwekar. Biological activities of leaves of ethnomedicinal plant, Borassus flabellifer Linn.(Palmyra palm): An antibacterial, antifungal and antioxidant evaluation. Bulletin of Faculty of Pharmacy, Cairo University 54 (1), 59-66.
39. SL Patwekar, SR Pedewad, S Gattani. Development and evaluation of nanostructured lipid carriers-based gel of isotretinoin. Particulate Science and Technology 36 (7), 832-843.
40. PP Sambarkar, SL Patwekar, BM Dudhgaonkar. Polymer nanocomposites: An overview. Int J Pharm Pharm Sci 4 (2), 60-65.
41. SL Patwekar. Nanobiocomposite: A new approach to drug delivery system. Asian Journal of Pharmaceutics (AJP) 10 (04).
42. PM Dhere, SL Patwekar. Review on preparation and evaluation of oral disintegrating films. Int J Pharm Tech 3 (4), 1572-1585.
43. S Patwekar, S Gattani, R Giri, A Bade, B Sangewar, V Raut. Review on nanoparticles used in cosmetics and dermal products. World J. Pharm. Pharm. Sci 3, 1407-1421.
44. SA Payghan, VK Kate, K Khavane, SS Purohit. Pharmaceutical solid polymorphism: Approach in regulatory consideration. J Glob Pharm Technol 1, 45-53.
45. L Shailesh, RP Snehal, P Ashwini, S Manoj, B Arvind. Nanostructured lipid carriers in stability improvement for cosmetic nanoparticles. International Journal of Pharmacy & Pharmaceutical Resarch 6 (1), 168-180.
46. SL Patwekar, RS Sakhare, NN Nalbalwar. HPLC method development and validation-A general Concept. International Journal of Chemical and Pharmaceutical Sciences 6 (1), 8-14.
47. SPD V.N Gunjkar, S.L.Patwekar. Stimuli Responsive Layer By Layer Self-Assembly A Novel Approachs In Current Drug Delivery: Review. World Journal of Pharmacy And Pharmaceutical Sciences 4 (6), 216-238.
48. SL Patwekar. Solubility and dissolution enhancement of poorly water-soluble Ketoprofen by microwave-assisted Bionanocomposites: in vitro and in vivo study. Asian Journal of Pharmaceutics (AJP) 10 (04).
49. KA Nangare, SD Powar, VK Kate, SR Patwekar, SA Payghan. Therapeutics Applications of Nanosuspension in Topical/Mucosal Drug Delivery. Journal of Nanomedicine Research 7 (1).
50. K Khavane, V Addepalli, K Bhusare, SA Payghan, S Patweakar, V Kate. Prescribing patterns of antibiotics and sensitivity patterns of micro-organisms towards different antibiotics in multidisciplinary health care hospital. International Journal of Pharmaceutical and Biologic Archives 1 (2), 115-22.

51. SG Gattani, SL Patwekar. Enhancement solubility and dissolution Rate of Ibuprofen by Nanobiocomposites using Microwave Induced Diffusion (MIND) Method. World Journal Of Pharmacy and Pharmaceutical Sciences 6 (11), 716-740.
52. A Jirage, K Shaikh, K Vaishali, SA Payghan, S Patwekar. In vitro-in vivo correlation for poly (3-hydroxybutyrate) base ibuprofen extended release tablets. Asian J. Pharm 11, 18-26.
53. S Patwekar, G Gattani, R Sakhare, A Khan, S Gaikwad, S Pedewad. Current features of USFDA and EMA process validation guidance. Int. J. Pharm. Pharm. Res 6 (1), 300-313.
54. PG Jamkhande, SR Barde, SL Patwekar, PS Tidke. Plant profile, phytochemistry and pharmacology of Cordia dichotoma, 1009-16.
55. GV Gole, SL Patwekar, A Doiphode, A Rode, S Shaikh. A Overview on Nanosponges. A & V Publications 12 (3), 210-212.
56. L Mahajan, N Kapase Sachin, G Sonawane, S Barde, R Sakhare, R Moon. The Highlights On Herbs Acts As An Anti-Cancer Property–A Systematic Review. Natural Volatiles & Essential Oils Journal, 15692-15704.
57. VK Magar, L Sonawane, S Patwekar. Molecular Docking Study Of Few Novels Pyrimidine Derivatives On Validated Target Enoyl Acyl Coa Reductase. Latin American Journal of Pharmacy: A Life Science Journal 42 (3), 777-791.
58. SL Patwekar, G Namdev, V Gole, A Rode, S Shaikh. A Overview on Nanoemulsion. Asian Journal of Research in Pharmaceutical Sciences 12 (3), 239-244.
59. AR Doiphode, SL Patwekar, N Guhade, V Gole, A Rode, S Shaikh. A Overview on nanoemulsion. A & V Publications 12 (3), 239-244.
60. MRP Rao, S Taktode, SS Shivpuje, S Jagtap. Optimization of Transmucosal Buccal Delivery of Losartan Potassium using Factorial Design. Indian Journal of Pharmaceutical Education and Research, 2016; 50(2): S132-S139.
61. N Patre, S Patwekar, S Dhage, S Shivpuje. Formulation & Evaluation Of Piroxicam Bionanocomposite For Enhancement of Bioavailability. European Journal of Molecular & Clinical Medicine, 2020; 7(11): 9362-9376.
62. SJ Wadher, SL Patwekar, SS Shivpuje, SS Khandre, SS Lamture. Stability Indicating Assay Methods for Simultaneous Estimation of Amoxicillin Trihydrate And Cloxacillin Sodium in Combined Capsule Dosage Form by UV-Spectrophotometric Method. European Journal of Biomedical and Pharmaceutical sciences, 2017; 4(10): 858-864.
63. Santosh A. Payghan Shivraj S. Shivpuje Shailesh L. Patwekar, Karna B. Khavane, Padmavati R. Chainpure. A Review on Different Preparation Method Used For Development of Curcumin Nanoparticles. International Journal of Creative Research Thoughts, 2021;9(1):4088-4101.
64. Zeba Ashfaq Sheikh P. R. Chainpure, S. L. Patwekar, S. S. Shivpuje. Formulation and evaluation of Garciniacambogia and Commiphoramukul Herbal tablets used for AntiObesity. International Journal of Engineering, Science and Mathematics, 2019; 8(4): 180-195.
65. Pravin P Karle, Shashikant C Dhawale, Vijay V Navghare, Shivraj S Shivpuje. Optimization of extraction conditions and evaluation of Manilkara zapota (L.) P. Royen fruit peel extract for in vitro α-glucosidase enzyme inhibition and free radical scavenging potential. Future Journal of Pharmaceutical Sciences, 2021; 7(1):1-10.
66. Sheetal Rathod P. R. Chainpure, S. L. Patwekar, S. S. Shivpuje. A Study Of Carica Papaya Concerning It's Ancient And Traditional Uses - Recent Advances And Modern Applications For Improving The Milk Secretion In Lactating Womens. International Journal of Research, 2019;8(2):1851-1861.
67. Shivraj S. Shivpuje Shailesh J. Wadher, Bhagwan B. Supekar. Development And Validation Of New Ft-Ir Spectrophotometric Method For Simultaneous Estimation Of Ambroxol Hydrochloride

And Cetirizine Hydrochloride In Combined Pharmaceutical. International Research Journal of Pharmacy, 2019; 10(3):110-114.

68. Shivraj S. Shivpuje, Shailesh J. Wadher, Bhagwan B. Supekar. Simultaneous Estimation of Ambroxol Hydrochloride and Cetirizine Hydrochloride in Combined Solid Tablet Formulations by HPTLC- Densitometric Method. Asian Journal of Biochemical and Pharmaceutical Research, 2019; 9(1):1-10.
69. JW Sailesh, SS Shivraj, SI Liyakat. Development and Validation of Stability Indicating RP-HPLC Method for the Estimation of Simvastatin in Bulk and Tablet Dosage form. Research Journal of Pharmacy and Technology, 2018; 11(4): 1553-1558.
70. Patil S. S. Shivpuje Shivraj S. Patre Narendra G. Development and Validation Of Stability Indicating HPTLC Method For Determination of Nisoldipine (Niso) In Tablet Dosage Form. European Journal of Biomedical and Pharmaceutical sciences, 2017; 4(12):462468.
71. W Shailesh, K Tukaram, S Shivraj, L Sima, K Supriya. Development and Validation of Stability Indicating UV Spectrophotometric Method for Simultaneous Estimation of Amoxicillin Trihydrate and Metronidazole In Bulk And In-House Tablet. World Journal of Pharmaceutical and Medical Research, 2017;3(8):312-318.
72. J Wadher Shailesh, M Kalyankar Tukaram, S Shivpuje Shivraj. Development and Validation of Stability Indicating Assay Method for Simultaneous Estimation of Amoxicillin Trihydrate and Cloxacillin Sodium In Pharmaceutical Dosage Form By Using RP-HPLC. World Journal of Pharmaceutical Research, 2017; 10(6):1002-1006.
73. Shital S. Sangale, Priyanka S. Kale, Rachana B. Lamkane, Ganga S. Gore, Priyanka B. Parekar, Shivraj S. Shivpuje (2023). Synthesis of Novel Isoxazole Derivatives as Analgesic Agents by Using Eddy's Hot Plate Method. South Asian Res J Pharm Sci, 5(1): 18-27.
74. Priyanka B. Parekar, Shivraj S. Shivpuje, Vijay V. Navghare, Manasi M. Savale, Vijaya B. Surwase, Priti S. Mane- Kolpe, Priyanak S. Kale. Polyherbal Gel Development And Evaluation For Antifungal Activity, European Journal of Molecular & Clinical Medicine. 2022; 9(03): 5409-5418.
75. Jain AA, Mane-Kolpe PD, Parekar PB, Todkari AV, Sul KT, Shivpuje SS. Brief review on Total Quality Management in Pharmaceutical Industries, International Journal of Pharmaceutical Research and Applications. 2022; 7(05):1030-1036.
76. Sumaiyya. K. Attar, Pooja P. Dhanawade, Sonali S. Gurav , Prerna H. Sidwadkar , Priyanka B. Parekar, Shivraj S. Shivpuje. Development and Validation of UV Visible Spectrophotometric Method for Estimation of Fexofenadine Hydrochloride in Bulk and Formulation, GIS SCIENCE JOURNAL. 2022; 9(11): 936-944.
77. Sumayya Kasim Atar, Priyadarshini Ravindra Kamble, Sonali Sharad Gurav, Pooja Pandit Dhanawade, Priyanka Bhanudas Parekar, Shivraj Sangapa Shivpuje. Phytochemical Screening, Physicochemical Analysis of Starch from Colocasia Esculenta, NeuroQuantology, 2022; 20(20): 903-917.
78. Priti D.Mane-Kolpe, Alfa A. Jain, Tai P. Yele, Reshma B. Devkate, Priyanka B. Parekar, Komal T. Sul, Shivraj S. Shivpuje. A Systematic Review on Effects of Chloroquine as a Antiviral against Covid-19, International Journal of Innovative Science and Research Technology, 2022;7(11): 989-995.
79. Dr. Rohit Jadhav, Prof. Abhay D. Kale, Dr. Hitesh Vishwanath Shahare, Dr. Ramesh Ingole, Dr Shailesh Patwekar, Dr S J Wadher, Shivraj Shivpuje. Molecular Docking Studies and Synthesis of Novel 3-(3- hydroxypropyl)-(nitrophenyl)[1,3] thiazolo [4,5-d] pyrimidin2(3H)-one as potent inhibitors of P. Aeruginosa of S. Aureus, Eur. Chem. Bull. 2023; 12(12): 505-515.
80. Priyanka B. Parekar, Savita D. Sonwane, Vaibhav N. Dhakane, Rasika N. Tilekar, Neelam S. Bhagdewani, Sachin M. Jadhav, Shivraj S. Shivpuje, Synthesis and Biological Evaluationof Novel

1,3,4-Oxadiazole Derivatives as Antimicrobial Agents, Journal of Cardiovascular Disease Research, 2023; 14(8):611-624.

81. Kavita R. Mane, Prachi A. Ghadage, Aishwarya S. Shilamkar, Vaishnavi A. Pawar, Sakshi B. Taware, Priyanka B. Parekar, Shivraj S. Shivpuje. Phytochemical Screening, Extraction and In-vivo study of Immunomodulation effect of Withania somnifera, Momordicadioica and Annonasqumosa leaves. Journal of Cardiovascular Disease Research, 2023; 14(9): 231-241.
82. Harshada S. Deshmukh, Vishal B. Babar, Prajkta S. Jagtap, Rupendra V. Doshi, Shivarti V. Deokate, Ashwini V. Todkari, Amrata S. Mantri, Priyanka B. Parekar, Shivraj Shivpuje (2024). A Comprehensive Review Article on Herbal Cosmetics. South Asian Res J Pharm Sci, 6(3): 50-68.